Successive Attachment of Electrons to Protonated Guanine: $(G+H)^{\bullet}$ Radicals and $(G+H)^{-}$ Anions

Jun D. Zhang, Yaoming Xie, and Henry F. Schaefer, III*

Center for Computational Chemistry, University of Georgia, Athens, Georgia 30602-2525

Received: June 3, 2006

The structures, energetics, and vibrational frequencies of nine hydrogenated 9H-*keto*-guanine radicals $(G+H)^{\bullet}$ and closed-shell anions $(G+H)^{-}$ are predicted using the carefully calibrated (*Chem. Rev.* **2002**, *102*, 231) B3LYP density functional method in conjunction with a DZP++ basis set. These radical and anionic species come from consecutive electron attachment to the corresponding protonated $(G+H)^{+}$ cations in low pH environments. The $(G+H)^{+}$ cations are studied using the same level of theory. The proton affinity (PA) of guanine computed in this research (228.1 kcal/mol) is within 0.7 kcal/mol of the latest experiment value. The radicals range over 41 kcal/mol in relative energy, with radical **r1**, in which H is attached at the C8 site of guanine, having the lowest energy. The lowest energy anion is **a2**, derived by hydride ion attachment at the C2 site of guanine. No stable N2-site hydride should exist in the gas phase. Structure **a9** was predicted to be dissociative in this research. The theoretical adiabatic electron affinities (AEA), vertical electron affinities, and vertical detachment energies were computed, with AEAs ranging from 0.07 to 3.12 eV for the nine radicals.

Introduction

The initial step in DNA radiation damage is known to involve the interaction between ionizing sources (photons, electrons, and chemical radicals) and the polynucleotide. The intermediates resulting from electron trapping on nucleic acid bases,[1] identified as charged radicals, will cause further DNA lesions such as strand breaks,[2] base pair mutations,[3] and interstrand cross-links.[4] These lesions, if not repaired, may lead to lethal living cell damage. Thus, a reliable and comprehensive understanding of these transient radicals may shed light on the damage recognition processes and repair mechanisms. The base-centered radicals play a key role in the modified nucleobase formation processes when normal pyrimidine and purine base molecular structures alternate.[5] In recent investigations, guanine has been a focus, due to its having the highest propensity of reduction among the four bases.[6] Single guanine or guanine sequences have been detected as hole (radical cation) trapping sites in DNA strand charge transport experiments.[7] The 8-oxo-guanine molecule, which is the usual guanine oxidation product, has been the subject of great interest due to its mispairing ability with adenine (A) and cytosine (C).[8] Recent research has also shown that the electron capturing probability scales with the number of guanines in a single strand DNA oligomer.[9] Theoretical studies of gas-phase anionic guanine have demonstrated that guanine tautomers have near zero electron affinities, whether the end product is the dipole bound or valence bound anion.[10]

In acid environments, the interaction between protons and guanine may be attributed to the simple acid−base chemical equilibrium, both in the gas phase and condensed phases. Guanine has been recognized as the most readily protonated base, due to it having the highest proton affinity (PA) among the four DNA nucleobases.[11] The site specific PAs and pK_a values of guanine have been studied extensively.[12−14] Gas-phase data for the proton affinity of guanine has been obtained from Greco and co-workers'[11] FAB-MS (Fast Atom Bombardment Tandem Mass Spectrometry) experiments. In 2000, Podolyan, Gorb, and Leszczynski[13] preformed comprehensive theoretical studies to determine the gas-phase PAs of various nucleobases using post-Hartree−Fock methods. More recently, the absolute pK_a values of guanine in water have been predicted by Jang, Goddard, and co-workers.[14]

Despite the different methods used, all investigations have indicated that the N7 site protonated guanine (see Scheme 1) is the dominating form among the possible tautomers. However, previous investigations have not considered the possibility that protonated guanine tautomers may be electron trapping sites, in which the radical or anionic guanine−hydrogen complex may be formed after consecutive attachment of electrons to protonated guanine. The resulting guanine derivative species, classified as hydrogenated guanine radicals or anions, may lead to permanent DNA lesions. This is because the added hydrogen atom is covalently bound to guanine, except for protonated guanine, where the proton may be appended to the induced dipole of guanine. In the gas phase, the hydrogenated guanine radicals have been examined in Wetmore, Boyd, and Eriksson's EPR/ENDOR experiments and DFT computations.[15] The neutral and anionic states of the dehydrogenated guanine isomers have been studied by Luo and co-wokers.[16]

We focus here on the radicals $(G+H)^{\bullet}$ and anions $(G+H)^{-}$ formed by electrons attaching to protonated 9H-*keto*-guanine $(G+H)^{+}$ cations in the gas phase. The molecular structures and thermodynamic properties of all species have been predicted by using a carefully calibrated theoretical approach B3LYP/DZP++. The aim of this research is to complement the previous work on base-centered DNA radicals ((base−H)$^{\bullet}$ and (base+H)$^{\bullet}$)[16,17] and contribute to the studies of induced DNA fragment damage by low energy electron attachment in the gas phase.[18] Thus, we do not incorporate solvent effects in our theoretical approach. The structure and numbering scheme of

* Corresponding author. E-mail: hfs@uga.edu.

10.1021/jp0634454 CCC: $33.50
Published on Web 10/10/2006

SCHEME 1

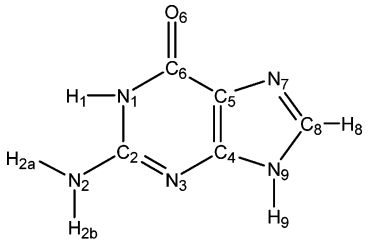

Guanine

guanine used in this work are depicted in Scheme 1 (showing the IUPAC numbering of the atoms).

In Scheme 1, as a building block of DNA, the 9H-*keto*-guanine molecule (ordinary guanine) connects the furanose sugar through the glycosidic bond at the N9 position. The guanine *enol* tautomers were not considered in this research, since they are less important biochemically compared to 9H-*keto*-guanine. An understanding of molecular structures and energetic features of these critical molecules will help us to understand more complex DNA fragments.

Theoretical Methods

A carefully calibrated DFT approach[19] has been used in this research to optimize the many geometries and to predict vibrational frequencies. The method chosen is B3LYP, a combination of the exchange treatment from Becke's three parameter HF/DFT exchange functional (B3)[20] with the dynamic correlation functional of Lee, Yang, and Parr (LYP).[21] The Gaussian 94 system of DFT programs was used for the computations.[22] All computations were performed using double-ζ quality basis sets with polarization and diffuse functions (DZP++). The DZP++ basis sets were constructed by augmenting the Huzinage−Dunning set of contracted double-ζ Gaussian functions with one set of p-type polarization functions for each H atom and one set of five d-type polarization functions for each C, N, and O atom [$\alpha_p(H) = 0.75$, $\alpha_d(C) = 0.75$, $\alpha_d(N) = 0.80$, $\alpha_d(O) = 0.85$].[23,24] To complete the DZP++ basis, one even tempered diffuse s function was added to each H atom while sets of even tempered diffuse s and p functions were centered on each heavy atom. The even tempered orbital exponents were determined by the convention of Lee and Schaefer.[25]

The final DZP++ set contains six functions per H atom (5s1p/3s1p) and nineteen functions per C, N, or O atom (10s6p1d/5s3p1d), yielding a total of 245 contracted Gaussian functions for each (G+H)• hydrogenated base radical. This basis set has a significant tactical advantage, since it has been systematically examined in comprehensive calibrative studies of a wide range of electron affinities with average errors less than 0.12 eV for the case of a closed-shell anion and the corresponding open-shell neutral.[19]

The electron affinities were determined in the following manner. The adiabatic electron affinity (AEA) is defined as the energy difference between the neutral and corresponding anion species at their respective optimized geometries

$$\mathrm{AEA} = E(\text{optimized neutral}) - E(\text{optimized anion})$$

The vertical electron affinity (VEA) of the radical is defined as

$$\mathrm{VEA} = E(\text{optimized neutral}) - E(\text{anion at optimized neutral geometry}).$$

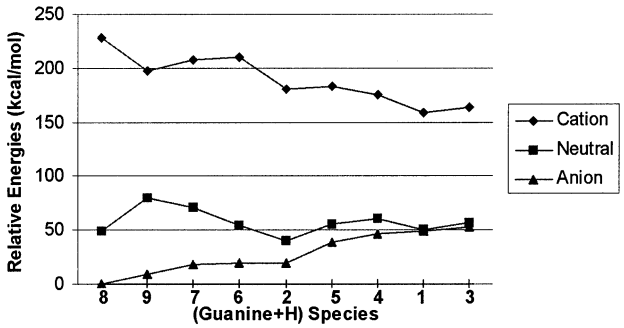

Figure 1. Relative energies of $(G+H)^+$, (G+H)•, and $(G+H)^-$ derived from guanine (G).

SCHEME 2

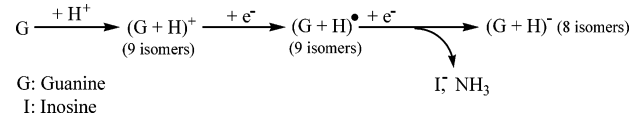

SCHEME 3

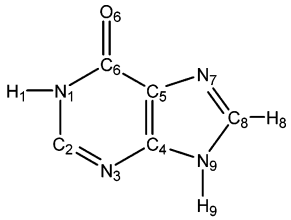

2-Dehydrogenated Inosine (I-H)

The anion vertical detachment energy (VDE) is determined via

$$\mathrm{VDE} = E(\text{neutral at optimized anion geometry}) - E(\text{optimized anion}).$$

To analyze the unpaired electron distributions, Kohn−Sham molecular orbitals and spin density plots were constructed from the appropriate B3LYP/DZP++ density. Natural population atomic (NPA) charges were determined using the natural bond order (NBO) analysis of Reed and Weinhold.[26−29]

Results and Discussion

The proposed reaction path for consecutive electron attachment to $(G+H)^+$, leading to the formation of hydrogenated guanine neutrals (G+H)• and anions $(G+H)^-$, is represented in Scheme 2.

We considered nine different protonated guanine isomers (**c1**−**c9**; these isomers are labeled in order of increasing energy) in the present research, involving the different heavy atoms of guanine as proton acceptors. The neutral (**r1**−**r9**) and anionic (**a1**−**a9**) forms of these structures may be envisioned as having been formed following electron attachment (neutrals and anions are labeled in the same manner as the corresponding cations). The relative energies of cation, radical and anion are shown in Figure 1. Eight of the nine isomers display anionic structure, whereas anion **a9** has been found to be a dissociative complex. In what follows, we will focus the present research on understanding the thermodynamic properties of these neutral and charged species, as well as those of the complex of 2-dehydrogenated inosine (Scheme 3) anion $(I - H)^-$ with ammonia (NH_3).

Vibrational frequencies were employed to characterize all optimized geometrical structures as stationary points on the potential energy surfaces.

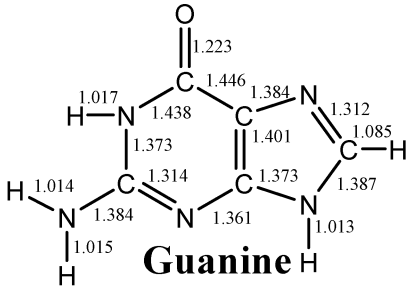
Guanine

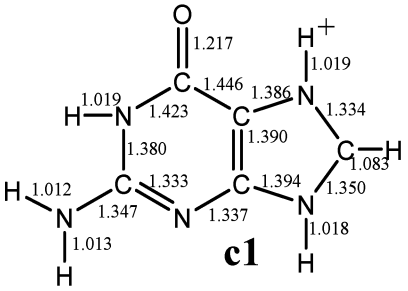
c1

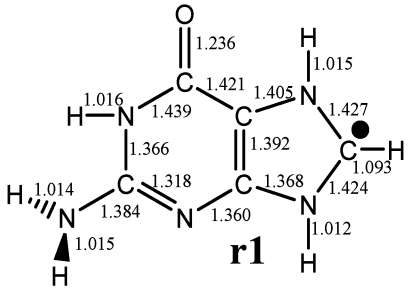
r1

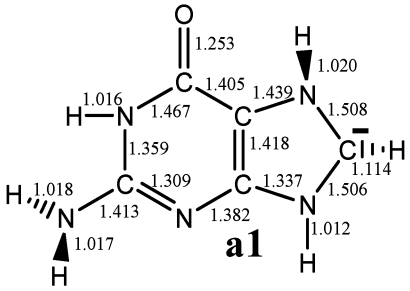
a1

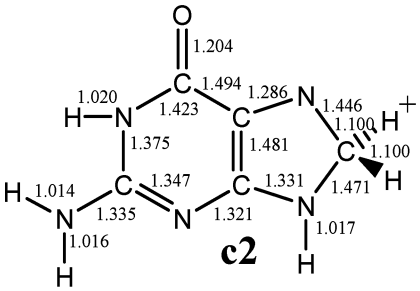
c2

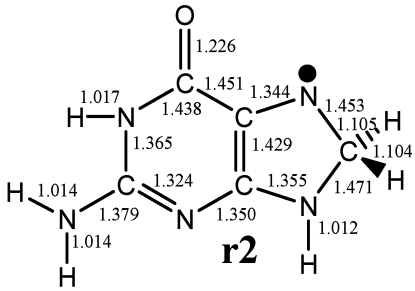
r2

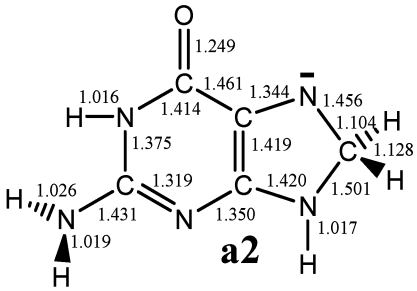
a2

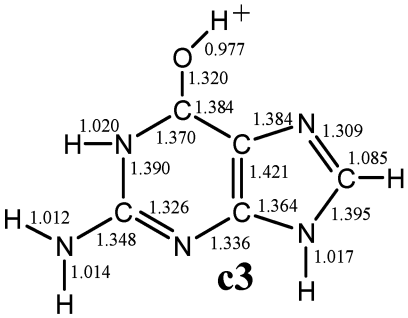
c3

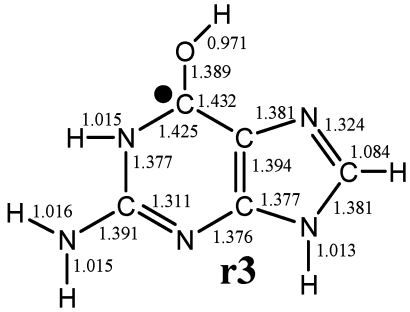
r3

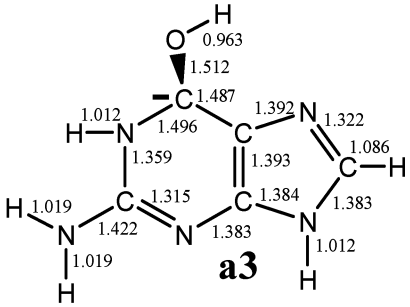
a3

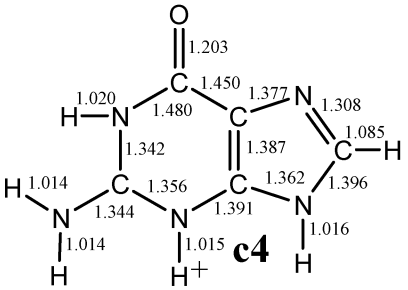
c4

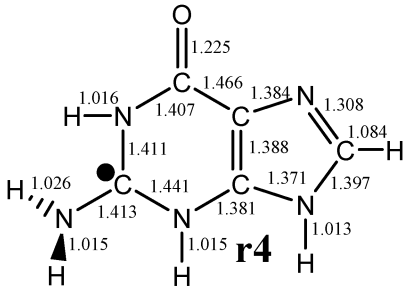
r4

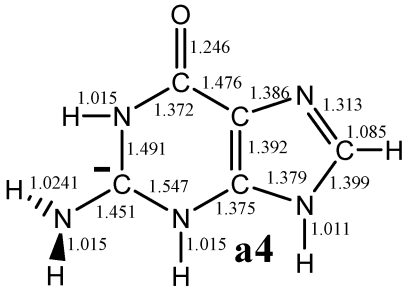
a4

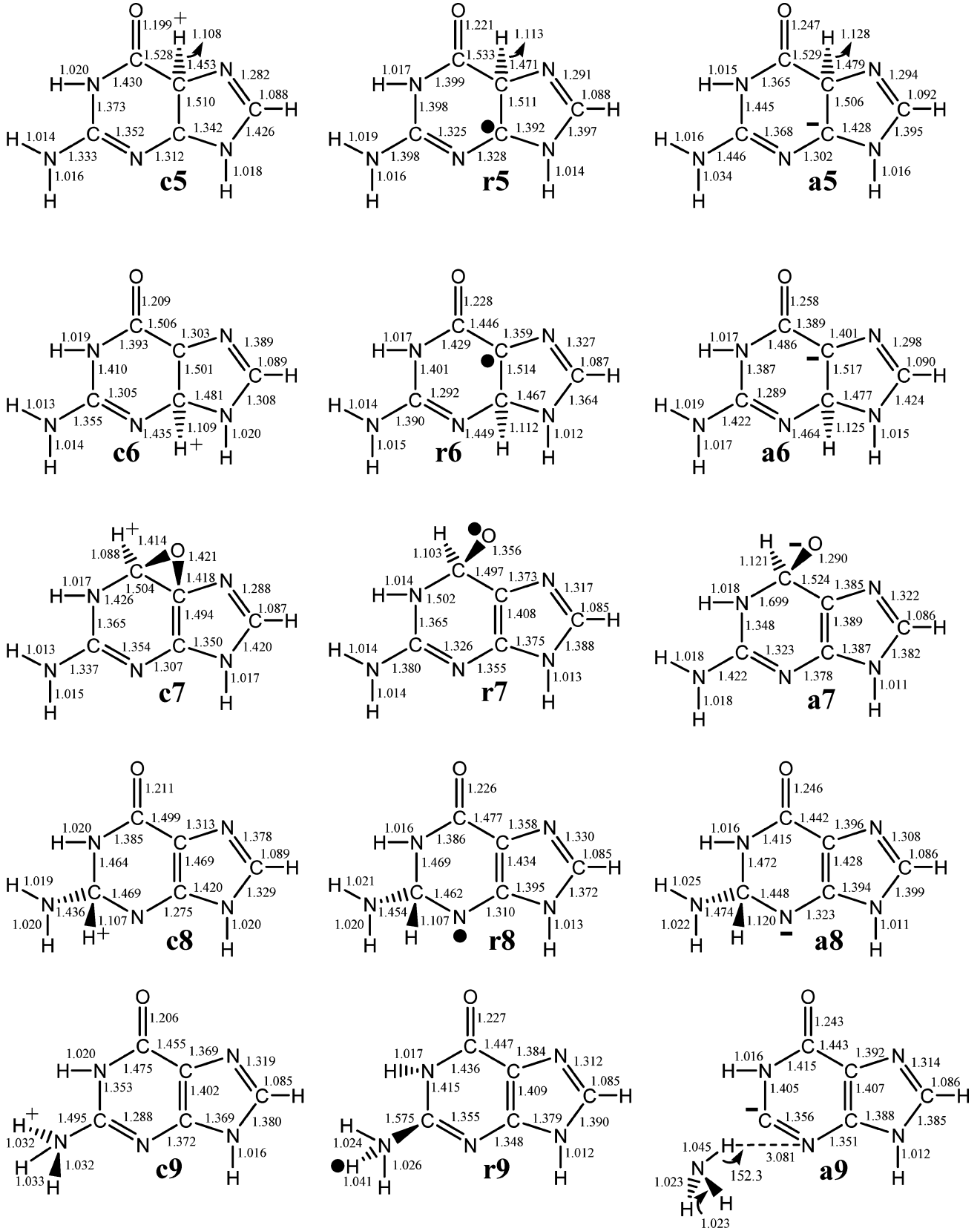

Figure 2. Geometries of guanine and the species $(G+H)^+$, $(G+H)^•$, and $(G+H)^-$ at the B3LYP/DZP++ level.

1. $(G+H)^+$ Cations and the Proton Affinities of Guanine. The formation of protonated guanine $(G+H)^+$ cations is directly related to the gas phase basicity of guanine. Generally, the proton is likely to attach to heavy atoms with lone pair electrons. The site specific proton affinities of guanine have been studied extensively.[11−14] The cation **c1** (Figure 2), associated with the appendage of a proton to atom N7 of guanine (Scheme 1), has its lowest energy on the potential energy surface, confirmed both theoretically and experimentally. The corresponding radical and anion isomers are labeled as **r1** and **a1**, respectively. The proton affinity of guanine leading to **c1** is computed as 228.1 kcal/mol in this research, in good agreement with the Greco's[11]

TABLE 1: Relative Energies of Protonated Guanine (G + H)$^+$ Structures and Proton Affinities (PA) in kcal/mol[a]

cations	relative energy	PA (with ZPVE) (B3LYP/DZP++)	PA (with ZPVE) (B3LYP/ 6-31++G)[12b]	exp't. PA[11]
c1	0.0	228.1	230	227.4 ± 0.1
c2	5.2	222.9	224	
c3	16.8	211.3	212	
c4	22.2	205.9		
c5	25.2	202.8		
c6	39.3	188.8	190	
c7	49.9	178.1		
c8	52.0	176.1		
c9	70.1	158.0		

[a] See Figure 2 for the labeling of the different protonated structures **c1**−**c9**.

TABLE 2: Relative Energies of Radicals Derived from Guanine (G + H)•[a]

radicals	relative energies (kcal/mol)	ZPVE corrected relative energies (kcal/mol)	Boyd's[b] relative energies[15] (kcal/mol)
r2	0.0	0.0	0.0
r8	8.4	9.2	
r1	9.9	10.4	11.0
r6	13.6	13.9	14.8
r5	15.7	15.4	35.8[c]
r3	16.4	16.9	19.5
r4	20.4	20.9	21.6
r7	30.7	31.1	
r9	40.1	40.6	

[a] See Figure 2 for the labeling of the different radicals **r1**−**r9**. [b] B3LYP/6-311G(2df,p)//B3LYP/6-31G(d,p) results with ZPVE corrections using the Bauschlicher and Partridge[BP] scaling factor (0.9804). [c] This earlier reported structure is qualitatively different from that predicted in the present research.

FAB-MS (fast atom bombardment tandem mass spectrometry) gas-phase experiment, 227.4 ± 0.1 kcal/mol. The other eight cations, labeled as **c2**−**c9**, are also displayed in Figure 2. The relative energies and proton affinities of the nine cations at B3LYP/DZP++ level of theory are presented in Table 1. These results include ZPVE corrections.

2. (G+H)• Radicals. The (G+H)• radical structures may be imagined as arising from electrons being appended to the (G+H)$^+$ cations. The energetics associated with such electron capture range from 4.6 to 7.8 eV and are identical to the ionization potentials of the (G+H)• structure. The relative energies (with ZPVE corrections) of the resulting nine neutral radicals at the B3LYP/DZP++ level of theory are presented in Table 2. From the geometrical structures of the (G+H)• isomers displayed in Figure 2, it may be noticed that all isomers undergo a significantly geometric change when compared to corresponding (G+H)$^+$ structures. The present energetic ordering of (G+H)• may be compared to the results of Wetmore, Boyd, and Eriksson at the B3LYP/6-311G(2df,p)//B3LYP/6-31G(d,p) level of theory[15] (Table 2). In Wetmore's work, their ordering qualitatively agrees with our findings except for the radical **r5**, which they predict to be a ring open structure with higher energy (20 kcal/mol) than that found in our studies.

Structure **r2** has the lowest total energy, and this radical arises from hydrogen atom addition to the C8 site. The N7−C8 bond length increases significantly from 1.312 Å in neutral guanine and 1.446 Å in **c2** to 1.453 Å for **r2**. The energetic favorability of the **r2** radical may be due to the conjugation between the radical center N7 and the neighboring double bond C4═C5, as shown in Scheme 4. The spin density distributions are positive for both the N7 (0.53) and C4 (0.16) sites. A similar conjugation

SCHEME 4

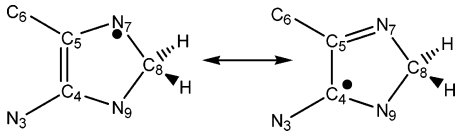

scheme may occur for radical **r8**, which is about 9.2 kcal/mol (ZPVE corrected) above the global minimum **r2** at the B3LYP/DZP++ level. The unpaired electron is has significant contributions from N3, C5, and C8, with spin densities 0.46, 0.38, and 0.26, respectively.

Radical **r1** lies 10.4 kcal/mol above the global minimum **r2**. The unpaired electron is mainly localized on the C8 atom with a spin density of 0.74. This radical is of potential biological importance because it may be an intermediate in the formation of 8-oxo-guanine. Radicals **r6** and **r5** are predicted to lie 13.9 and 15.4 kcal/mol, respectively, above the global minimum **r2** in the gas phase. The two species undergo significant geometrical distortions on formation compared to the planar guanine molecule. Sevilla[30] described these structures as "butterfly" conformations, in which the pyrimidine and imidazole rings remain planar but both are tilted about the C4−C5 bond. The spin density for radical **r6** is predicted to reside primarily on the C5 (0.50) and C8 (0.25) atoms and that for **r5** resides in large part on C4 (0.42) and C2 (0.34), due to the conjugation effects discussed above.

The radical **r4** is predicted to lie 20.9 kcal/mol higher than **r2**. The significant structural feature of this radical is that the N2 amino group is out-of-plane (following hydrogen atom addition) compared to closed-shell neutral guanine. There are two radical isomers arising from the hydrogen atom addition to the carbonyl group of guanine. These are **r3** associated with the hydrogen attached to atom O6 and **r7** with the additional hydrogen atom on C6. The total energy of **r3** is 16.9 kcal/mol higher than that of the global minimum **r2**. The resulting hydroxyl group is significantly out of the ring plane (by about 35°; the O6−C6−C5−C4 dihedral angle is 145.2°) due to the pyramidization of C6. Radical **r7** is the isomer with 31.1 kcal/mol higher than **r2**. Hydrogen atom addition to C6 results in an oxygen atom centered radical, comparable to that predicted to have the highest total energy for hydrogenated cytosine.[17c] Radical **r9** is the isomer with the highest total energy, namely 40.6 kcal/mol higher than **r2**. Hydrogen addition to the amino group causes the C2−N2 bond distance to increase significantly by 0.191 Å compared with neutral guanine.

3. (G+H)$^-$ Anions and the (I−H)$^-$···NH$_3$ Complex. We are the first to report the anionic structures for the hydrogenated guanine isomers. The eight open-shell neutral (G+H)• isomers (**r1**−**r8**), may form closed-shell anions (G+H)$^-$ upon capturing electrons. Radical **r9** is predicted to extrude NH_3 leading to a 2-dehydrogenated inosine (Scheme 3) anion and an ammonia molecule following electron attachment in the gas phase. The predicted geometrical structures of all anions are displayed in Figure 2 (labeled as **a1**−**a9**), and the relative energies (ZPVE corrected) are reported in Table 3. Only the conventional closed-shell singlet state anions are considered in this research. Figure 2 shows that adding one electron to the neutral radicals leads to significant geometrical changes, confirming that all anions are of distinctly covalent character.

It is shown in Table 2 that the energetic order of the anions differs significantly from that of the analogous radicals. Anion **a8** is the most favored energetically. The anion **a9**, with C_s symmetry, is a complex of 2-dehydrogenated inosine anion with ammonia. As the hydrogen donor, the ammonia forms a very

TABLE 3: Relative Energies of Anions Derived from Guanine (G+H)⁻ at the B3LYP/DZP++ Level[a]

anions	relative energy (kcal/mol)	ZPVE corrected relative energy (kcal/mol)	ZPVE corrected guanine hydride affinities (kcal/mol)
a8	0.0	0.0	51.8
a9	10.8	8.6	43.2
a7	18.9	17.9	33.9
a6	19.4	19.0	32.8
a2	20.6	19.5	32.3
a5	40.5	39.1	12.7
a4	46.9	46.0	5.8
a1	50.0	48.6	3.2
a3	53.7	52.5	−0.7

[a] See Figure 2 for the labeling of the different anions **a1**−**a9**.

SCHEME 5

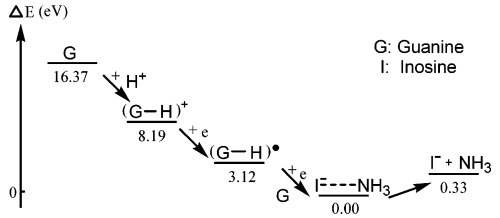

weak hydrogen bond with the inosine N3 atom, which has a −0.70 negative charge in the NBO analysis. The very long H_a•••N3 hydrogen bond distance is 3.081 Å, and the bond angle $N_a-H_a\cdots$N3 is 152.3°. The distance between H_a with inosine C2 atom is 2.165 Å, represented as a plausible hydrogen bond pattern $N_a-H_a\cdots$C2, since the C2 atom has a positive charge with 0.11 "electrons" from the NBO analysis. Scheme 5 shows the relative energies profile of guanine, protonated guanine **c9**, hydrogenated guanine **r9**, the inosine-ammonia complex **a9,** and the energy when inosine and ammonia are separated infinitely. The theoretical results presented here should contribute to the understanding of guanine deamination reaction mechanisms via consecutive electron attachment to protonated guanine in the gas phase.

The anions **a7**, **a6**, and **a2** lie in a narrow energy range 18−20 kcal/mol above the global minimum. A large energy difference (20 kcal/mol) between these three anions and remaining four anions, namely **a5**, **a4**, **a1**, and **a3**, is predicted in the gas phase at the B3LYP/DZP++ level theory. Accordingly, these four anions are predicted to lie 40−53 kcal/mol above the global minimum **a8** energetically.

4. Electron Affinities of (G+H)• and Vertical Detachment Energies of (G+H)⁻. Three kinds of neutral-anion energy separations, namely the adiabatic electron affinities (AEA with and without ZPVE corrections), the vertical electron affinities (VEA), and the vertical detachment energies (VDE), are reported in Tables 4 and 5. Compared to the AEA values for the earlier studied dehydrogenated guanine radicals (AEA ranges from 2.22 to 2.97 eV for five isomers),[16] the electron affinities for the hydrogen addition radicals lie in a broader range (AEAs range from 0.07 to 3.12 eV for nine isomers with ZPVE). The **r9** radical studied here has the largest AEA (3.12 eV), whereas **r1** has a nearly zero AEA value 0.07 eV, indicating that radical **r1** has a very low propensity to bind an electron. The theoretical VEA and VDE values are quite different from the adiabatic electron affinities (see Figure 3), due to the considerable geometrical changes between the radicals (G+H)• and the corresponding anions (G+H)⁻. Compared to the AEA value, the VEA of **r9** is quite small (0.60 eV). This is because the optimized neutral geometrical structure is significantly different from the optimized anionic complex structure.

TABLE 4: Electron Attracting Properties of (G + H)•[a]

	adiabatic electron affinity (eV)		
radicals	AEA	ZPVE corrected AEA	vertical electron affinity (eV)
r1	−0.01	0.07	−0.47
r3	0.12	0.19	−0.51
r4	0.58	0.64	0.11
r5	0.65	0.70	0.15
r2	0.84	0.88	0.49
r6	1.48	1.51	1.11
r8	2.10	2.13	1.90
r7	2.24	2.30	1.65
r9	3.00	3.12	0.60

[a] See Figure 2 for the Labeling of the Different Radicals **r1**-**r9**.

TABLE 5: Electron Ejecting Properties of (G+H)⁻[a]

anions	vertical electron detachment energies (eV)
a1	1.06
a3	1.20
a2	1.21
a5	1.23
a4	1.25
a6	1.83
a8	2.30
a7	2.72
a9	3.18

[a] See Figure 2 for the labeling of the different anions a1−a9.

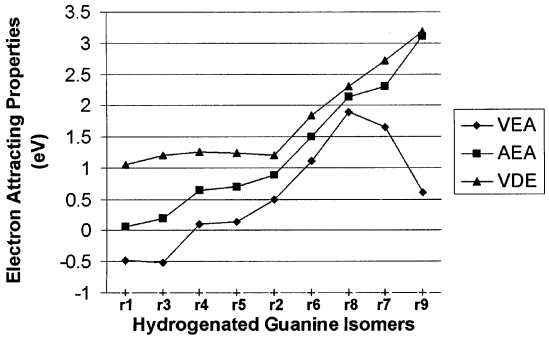

Figure 3. Electron attracting properties for (G+H)• and (G+H)⁻ derived from guanine.

Results and Discussion

In the present work, 27 hydrogenated guanine isomers in cationic, neutral, and anionic states have been studied theoretically. The structures, energetics, and theoretical electron affinities are predicted using the carefully calibrated[19] B3LYP density functional method in conjunction with DZP++ basis sets. Our main findings include the following.

1. The computational results for nine protonated guanine cations are compared with experiment and with previous theoretical studies. The proton affinity of **c1** quantitatively matches the latest gas phase experimental measurement, within 1 kcal/mol. Protons are found likely to bind on the nitrogen and oxygen sites of guanine with an energetic range of 39 kcal/mol, whereas the guanine carbon sites are less favorable to protonation, since the energies range as high as 70 kcal/mol (Table 1).

2. Nine neutral hydrogenated guanine radicals have been examined. Radical **r2**, with the H atom attached at the guanine C8 site, is predicted to be the global minimum on the potential energy surface. Radical **r9**, with the additional hydrogen atom at N2, has the highest energy, namely 40.6 kcal/mol above **r2** (Table 2).

3. The energetic order for the anions differs from that of the analogous radicals (Table 3, Figure 1). The global minimum among all the anion structures is **a8**, associated with a hydride ion at the guanine C2 position. Eight of the nine anions are valence bound and should be stable species in the gas phase. Structure **a9** is a deaminated guanine (C2-dehydrogenated inosine) anion/neutral ammonia complex, which is only 8.6 kcal/mol higher than **a8**. The significant geometry changes from **r9** (neutral) to **a9** (anion) explain the low VEA value (0.60 eV) of **r9** (Figure 3).

4. The geometrical distortions of $(G+H)^+$, $(G+H)^\bullet$, and anions $(G+H)^-$ with respect to ordinary guanine includes ring distortion, amino group pyramidalization, and the "butterfly" shape noted by Sevilla.[30] Generally, the $(G+H)^+$ minima favor the planar geometrical structures. The $(G+H)^-$ anions exhibit the largest geometrical distortions.

5. Among the hydrogenated guanine radicals, the carbon-centered formal radicals have the lowest AEA values (average 0.62 eV), whereas the two nitrogen-centered formal radicals have mid AEA values (average 1.59 eV), and the oxygen-centered formal radical **r7** has a 2.24 eV AEA value. The appearance of diverse AEA values related to different-centered radicals is one of the most fundamental elements of this research.[17]

6. The present study indicates that $(G+H)^\bullet$ and $(G+H)^-$ readily exist as the products of consecutive electron attaching to $(G+H)^+$. The different energetic orderings for the $(G+H)^+$, $(G+H)^\bullet$, and $(G+H)^-$ structures (Figure 1) imply that there may exists intramolecular hydrogen atom transfer among the different isomers during the electron attachment processes.

Acknowledgment. We appreciate the generous support of the U.S. National Science Foundation, Grant CHE-0451445.

References and Notes

(1) (a) O'Neill, P.; Fielden, M. *Adv. Radiat. Biol.* **1993**, *17*, 53−120 (b) Becker, D.; Sevilla, M. D. *Adv. Radiat. Biol.* **1993**, *17*, 121−131 (c) Colson, A. O.; Sevilla, M. D. *Int. J. Radiat. Biol.* **1995**, *67*, 627 (d) Sanche, L. *Mass Spectrom. Rev.* **2002**, *21*, 349. (e) Kelly, S. O.; Barton, J. K. *Science* **1999**, *283*, 375. (f) Ratner, M. *Nature* **1999**, *397*, 480. (g) Huels, M. A.; Hahndorf, I.; Illenberger, E.; Sanche, L. *J. Chem. Phys.* **1998**, *108*, 1309.

(2) (a) Cai, Z.; Dextraze, M.; Cloutier, P.; Hunting, D.; Sanche, L. *J. Chem. Phys.* **2006**, *124*, 024705. (b) Purkayastha, S.; Bernhard, W. A. *J. Phys. Chem. B* **2004**, *108*, 18377. (c) Li, X.; Sevilla, M. D.; Sanche, L. *J. Am. Chem. Soc.* **2003**, *5*, 13668. (d) Karagiannis, T. C.; El-Osta, A. *Cell. Mol. Life Sci.* **2004**, *61*, 2137.

(3) (a) Llano, J.; Eriksson, L. A. *Phys. Chem. Chem. Phys.* **2004**, *6*, 4707. (b) Cater, K. N.; Greenberg, M. M. *J. Am. Chem. Soc.* **2003**, *125*, 13376. (c) Cai, Z.; Sevilla, M. D. *Radiat. Res.* **2003**, *159*, 411.

(4) (a) Hong, I. S.; Greenberg, M. M. *J. Am. Chem. Soc.* **2005**, *127*, 3692. (b) Hong, I. S.; Ding, H.; Greenberg, M. M. *J. Am. Chem. Soc.* **2006**, *128*, 2230.

(5) (a) Abdoul-Carime, H.; Cloutier, P.; Sanche, L. *Radiat. Res.* **2001**, *155*, 625. (b) Huels, M. A.; Boudaiffa, B.; Cloutier, P.; Hunting, D.; Sanche, L. *J. Am. Chem. Soc.* **2003**, *125*, 4467. (c) Abdoul-Carime, H.; Gohlke, S.; Illenberger, E. *Phys. Rev. Lett.* **2004**, *92*, 168103.

(6) (a) Pullman, B.; Pullman, A. *Proc. Natl. Acad. Sci. U.S.A.* **1958**, *44*, 1197. (b) Lin, J.; Yu, C.; Peng, S.; Akiyami, I.; Li, K.; Lee, L. K.; LeBreton, P. R. *J. Phys. Chem.* **1980**, *84*, 1006. (c) Steenken, S.; Jovanovic, S. V. *J. Am. Chem. Soc.* **1997**, *119*, 617.

(7) (a) Giese, B. *Acc. Chem. Res.* **2000**, *33*, 631. (b) O'Neill, M. A.; Barton, J. K. *J. Am. Chem. Soc.* **2004**, *126*, 11471. (c) Lewis, F. D. *Photochem. Photobiol.* **2005**, *81*, 65. (d) Schuster, G. B. *Acc. Chem. Res.* **2000**, *33*, 253.

(8) (a) Cadet, J.; Delatour, T.; Douki, T.; Gasparutto, D.; Pouget, J. P.; Sauvaigo, S. *Mutat. Res.* **1999**, *424*, 9. (b) Bruner, S. D.; Norman, D. P. G.; Verdine, G. C. *Nature* **2000**, *403*, 859. (c) Ober, M.; Linne, U.; Gierlich, J.; Carell, T. *Angew. Chem., Int. Ed.* **2003**, *42*, 4947. (d) Cheng, X.; Kelso, C.; Hornak, V.; de los Santos, C.; Grollman, A. P.; Simmerling, C. *J. Am. Chem. Soc.* **2005**, *127*, 13906. (e) Jena, N. R.; Mishra, P. C. *J. Phys. Chem. B* **2005**, *109*, 14205.

(9) Ray, S. G.; Daube, S. S.; Naaman, R. *Proc. Natl. Acad. Sci. U.S.A.* **2005**, *102*, 15.

(10) (a) Roehrig, G. H.; Oyler, N. A.; Adamowicz, L. *Chem. Phys. Lett.* **1994**, *225*, 265. (b) Wetmore, S. D.; Boyd, R. J.; Eriksson, L. A. *Chem. Phys. Lett.* **2000**, *322*, 129. (c) Wesolowski, S. S.; Leininger, M. L.; Pentchev, P. N.; Schaefer, H. F. *J. Am. Chem. Soc.* **2001**, *123*, 4023. (d) Li. X.; Cai, Z.; Sevilla, M. D. *J. Phys. Chem. A* **2002**, *106*, 1596. (e) Haranczyk, M.; Gutowski, M. *J. Am. Chem. Soc.* **2005**, *127*, 699.

(11) Greco, F.; Liguori, A.; Sindona G.; Uccella, N. *J. Am. Chem. Soc.* **1990**, *112*, 9092.

(12) (a) Steenken, S. *Chem. Rev.* **1989**, *89*, 503. (b) Reynisson, J.; Steenken, S. *Phys. Chem. Chem. Phys.* **2002**, *4*, 527. (c) Giese, B.; McNaughton, D. *Phys. Chem. Chem. Phys.* **2002**, *4*, 5161.

(13) Podolyan, Y.; Gorb, L.; Leszczynski, J. *J. Phys. Chem. A* **2000**, *104*, 7346.

(14) Jang, Y. H.; Goddard, W. A.; Noyes, K. T.; Sowers, L. C.; Hwang, S.; Chung, D. S. *J. Phys. Chem. B* **2003**, *107*, 344.

(15) Wetmore, S. D.; Boyd, R. J.; Eriksson, L. A. *J. Phys. Chem. B* **1998**, *102*, 9332.

(16) Luo, Q.; Li, Q. S.; Xie, Y.; Schaefer, H. F. *Collect. Czech. Chem. Commun.* **2005**, *70*, 6.

(17) (a) Evangelista, F. A.; Paul, A.; Schaefer, H. F. *J. Phys. Chem. A* **2004**, *108*, 3565. (b) Luo, Q.; Li, J.; Li, Q. S.; Kim, S.; Wheeler, S. E.; Xie, Y.; Schaefer, H. F. *Phys. Chem. Chem. Phys.* **2005**, *6*, 1. (c) Zhang, J. D.; Xie, Y.; Schaefer, H. F.; Luo, Q.; Li, Q. S. *Mol. Phys.* **2006**, in press.

(18) (a) Boudaiffa, B.; Cloutier, P.; Hunting, D.; Huels, M. A.; Sanche, L. *Science* **2000**, *287*, 1658. (b) Zhang, Y.; Cloutier, P.; Hunting, D.; Wagner, J. R.; Sanche, L. *J. Am. Chem. Soc.* **2004**, *126*, 1002. (c) Cai, Z.; Cloutier, P.; Hunting, D.; Sanche, L. *J. Phys. Chem. B* **2005**, *109*, 4796. (d) Barrios, R.; Skurski, P.; Simons, J. *J. Phys. Chem. B* **2002**, *106*, 7991. (e) Anusiewicz, I.; Berdys, J.; Sobczyk, M.; Skurski, P.; Simons, J. *J. Phys. Chem. A* **2004**, *108*, 11381. (f) Gu, J.; Xie, Y.; Schaefer, H. F. *J. Am. Chem. Soc.* **2006**, *128*, 1250.

(19) Rienstra-Kiracofe, J. C.; Tschumper, G. S.; Schaefer, H. F.; Nandi, S.; Ellison, G. B. *Chem. Rev.* **2002**, *102*, 231.

(20) Becke, A. D. *J. Chem. Phys.* **1993**, *98*, 5648.

(21) Lee, C.; Yang, W.; Parr, R. G. *Phys. Rev. B* **1988**, *37*, 785.

(22) Frisch, M. J.; Trucks, G. W.; Schlegel, H. B.; Scuseria, G. E.; Robb, M. A.; Cheeseman, J. R.; Zakrzewski, V. G.; Montgomery, J. A.; Stratmann, R. E.; Burant, J. C.; Dapprich, S.; Millam, J. M.; Daniels, A. D.; Kudin, K. N.; Strain, M. C.; Farkas, O.; Tomasi, J.; Barone, V.; Cossi, M.; Cammi, R.; Mennucci, B.; Pomelli, C.; Adamo, C.; Clifford, S.; Ochterski, J.; Petersson, G. A.; Ayala, P. A.; Cui, Q.; Morokuma, K.; Salvador, P.; Dannenberg, J. J.; Malick, D. K.; Rabuck, A. D.; Raghavachari, K.; Foresman, J. B.; Cioslowski, J.; Ortiz, J. V.; Baboul, A. G.; Stefanov, B. B.; Liu, G.; Liashenko, A.; Piskorz, P.; Komaromi, I.; Gomperts, R.; Martin, R. L.; Fox, D. J.; Keith, T.; Al-Laham, M. A.; Peng, C. Y.; Nanayakkara, A.; Challacombe, M.; Gill, P. M. W.; Johnson, B. G.; Chen, W.; Wong, M. W.; Andres, J. L.; Gonzalez, C.; Head-Gordon, M.; Replogle, E. S.; Pople, J. A. *Gaussian 94*, revision c.3; Gaussian, Inc.: Pittsburgh, PA, 1995.

(23) Huzinaga, S. *J. Chem. Phys.* **1965**, *42*, 1293.

(24) Dunning, T. H. *J. Chem. Phys.* **1970**, *53*, 2823.

(25) Lee, T. J.; Schaefer, H. F. *J. Chem. Phys.* **1985**, *83*, 1784.

(26) Reed, A. E.; Weinstock, R. B.; Weinhold, F. *J. Chem. Phys.* **1985**, *83*, 735.

(27) Reed, A. E.; Weinhold, F. *J. Chem. Phys.* **1985**, *83*, 1736.

(28) Reed, A. E.; Curtiss, L. A.; Weinhold, F. *Chem. Rev.* **1988**, *88*, 899.

(29) Reed, A. E.; Schleyer, P. R. *J. Am. Chem. Soc.* **1990**, *112*, 1434.

(30) Colson, A. O.; Sevilla, M. D. *J. Phys. Chem.* **1996**, *100*, 4420.